Huys *et al. EPJ Nonlinear Biomedical Physics* (2015) 3:8
DOI 10.1140/epjnbp/s40366-015-0022-4

EPJ Nonlinear Biomedical Physics
a SpringerOpen Journal

RESEARCH Open Access

Does changing Fitts' index of difficulty evoke transitions in movement dynamics?

Raoul Huys[1*], Hester Knol[1], Rita Sleimen-Malkoun[1,2], Jean-Jacques Temprado[2] and Viktor K. Jirsa[1]

* Correspondence:
raoul.huys@univ-amu.fr
[1]Institut de Neurosciences des Systèmes, INSERM UMR1106, Aix-Marseille Université, Faculté de Médicine, la Timone, 27 Bd Jean Moulin, 13005 Marseille, France
Full list of author information is available at the end of the article

Abstract

Background: The inverse relationship between movement speed and accuracy in goal-directed aiming is mostly investigated using the classic Fitts' paradigm. According to Fitts' law, movement time scales linearly with a single quantity, the index of difficulty (*ID*), which quantifies task difficulty through the quotient of target width and distance. Fitts' law remains silent, however, on how *ID* affects the dynamic and kinematic patterns (i.e., perceptual-motor system's organization) in goal-directed aiming, a question that is still partially answered only.

Methods: Therefore, we here investigated the Fitts' task performed in a discrete as well as a cyclic task under seven *IDs* obtained either by scaling target width under constant amplitude or by scaling target distance under constant target width.

Results: Under all experimental conditions Fitts' law approximately held. However, qualitative and quantitative dynamic as well as kinematic differences for a given *ID* were found in how the different task variants were performed. That is, while *ID* predicted movement time, its value in predicting movement organization appeared to be limited.

Conclusion: We conclude that a complete description of Fitts' law has yet to be achieved and speculate that the pertinence of the index of difficulty in studying the dynamics underlying goal-directed aiming may have to be reconsidered.

Keywords: Fitts' law; Goal-directed aiming; Dynamical systems; Sensorimotor control

PACS code: 87.19.rs (movement)

MCS code: 92B99

Background

More than 60 years ago, Paul Fitts initiated a novel paradigm when he asked participants to cyclically move a stylus between two targets characterized by a width W and separated by a distance D [1]. By systematically varying D and W, he found that movement time MT related linearly to the ratio of D and W, $MT = a + b \times \log_2 (2D/W)$. This linear relation, now known as Fitts' law, was next found to hold also for discrete aiming [2]. In Fitts' law, the index of difficulty $ID = \log_2 (2D/W)$ quantifies task difficulty as an informational quantity in bits [2, 3]. Over the years, several authors have voiced criticism as to the functional form of the scaling of MT with ID as well as on whether the ID as formulated by Fitts is the most appropriate one [4–8]. Regardless, few will debate that as a first approximation, MT scales linearly with the ID, which has been repeatedly shown in discrete and cyclical performances alike [9–13].

Fitts' law, however, is silent on how the movements' organization changes as the ID is scaled. In addressing this issue, one prominent class of models (sub-movement models) focuses on the presence and features of primary and corrective secondary (and sometimes more) sub-movements as a function of *W* and *D* [5, 6, 14]. The features associated with these movements, and those that deemed most relevant, are typically scalar variables (duration, [average] velocity, proportion of corrective movements, etc.).

Another prominent class of models (dynamical models) seeks to understand how the movements' kinematic and underlying dynamics change when *D* and/or *W* are systematically changed. In this case, the focus is geared towards trajectories in the Hooke's plane and/or phase space [11, 15, 16], and the identification of the dynamics as observable in the latter [17, 18]. In that regard, deterministic, autonomous, and time-continuous systems are unambiguously described by their flow in phase (or state) space (or vector field), i.e., the space spanned by the system's state variables [19]. For movements along a single physical direction, as in a (sliding) Fitts' task, it is commonplace to use the movement's position and its time-derivative velocity as the state variables [11, 20, 21] (but see [22, 23] for a critical discussion). The attractors that may live in such two-dimensional spaces are limited to (different kinds of) fixed points (i.e., points where velocity and acceleration are zero) and limit cycles (nonlinear closed orbits), which are associated with discrete and rhythmic movements, respectively [24, 25]. Changing the system's parameter(s) modifies the phase flow, and may evoke a bifurcation (i.e., a change in the system's solution(s)). If so, the parameter is referred to as a control or bifurcation parameter. Grounded in this latter perspective, the present study aimed to identify the dynamics, and further characterize the movements' kinematics, when changing the *ID* by varying *W* and *D* independently, in both discrete and cyclic versions of Fitts' task.

In that regard, for the cyclic Fitts' task version, it has been shown that gradually changing *ID* induces a gradual adjustment of the movement kinematics [11, 15], albeit less so when changing *D* than when changing *W*. In the latter case, the gradual adjustment may evoke an abrupt transition in the dynamics underlying the performance [17, 26] via a homoclinic bifurcation (i.e., from a limit cyclic dynamics to (two) fixed points, each having one stable and one unstable direction [i.e., saddles]); [17]). As hinted at, changing *ID* via target width *W* and distance *D* affects the aiming movement's velocity profiles differently [7, 11, 27]: increasing *D* mainly stretches the (bell-shaped) velocity profile, while increasing *W* renders it skewed (the deceleration phase lengthens relative to the acceleration phase). Thus, it is not clear if the scaling of *ID* per se induced the bifurcation in [17] or if effectively the manipulation of *W* did so. For discrete task performance, the pattern of kinematic changes as a function of *ID* (including the *D* and *W* differentiation) yields some similarities with those observed in the cyclic task version [12, 28]. The discrete and cyclic task, however, are fundamentally different in that, in the former but not the latter, movement velocity and acceleration must be zero before initiating the movement and upon ending it [10]. In this case, it seems self-evident to assume the existence of a fixed-point dynamics in the discrete task version. Various fixed-point dynamics scenarios, next to the above-mentioned connected saddles, are realizable, however. For instance, Schöner [25] has proposed that a fixed point (at location A) vanishes so as to temporally give way to a limit cycle—causing the movement, after which the limit cycle vanishes and the fixed point (at location B) re-occurs. Alternatively, a fixed point may be driven through phase space, more or less continuously changing the phase flow so that the system is 'dragged behind it" [29]. This scenario constitutes an interpretation of equilibrium point models

[30] in the framework of dynamical systems [31]. In this case, the trajectories in the phase space can be expected to be 'wiggly' and reveal little local convergence (i.e., overlaid trajectories can be expected to have a similar thickness throughout). Yet another possible realization involves a competition in which an active fixed point at location A vanishes while simultaneously another at location B comes into existence [29]. Indeed, while the discrete Fitts' task must involve fixed points, what remains unknown is: i) whether they are similar under *D* and *W* induced *ID* scaling, ii) if *ID* changes evoke a transition between mechanisms, and iii) if the fixed points assumed in the discrete task are the same as those found for the (*W* induced *ID* scaling) cyclic task. In fact, for the cyclic task, it is not known either if a transition occurs if *ID* is altered via target distance *D*. Teasing apart the contributions of *D* and *W* to the scaling of the *ID* will allow us to investigate whether *ID*, which plays a primordial role in the Fitts' paradigm, acts as bifurcation parameter or if effectively either *D* or *W* or both do so.

Based on the above reasoning, in the discrete task we predicted to observe fixed-point dynamics under all conditions. Under the distance manipulation, for low *ID,* the (average) velocity can be expected to be very low. We therefore expected to find indications for the existence of a driven fixed-point scenario. For the cyclic task, in line with previous findings we predicted to observe a bifurcation from a limit cycle dynamics to a fixed-point dynamics with decreasing target width [17]. Finally, we expected to find evidence either for a limit cycle dynamics or the driven fixed-point at small target distances and time-invariant fixed points at large target distances.

We examined our predictions primarily by investigating the underlying Fitts' task performance under discrete and rhythmic task versions and identifying bifurcations (if existent). In addition, to further characterize task performance, we also extracted various kinematic features of the movements. Thereto, we designed a Fitts' task that was performed in the discrete and cyclic mode, and in which task difficulty was scaled via *D* and *W* separately in different sessions. We found that while *ID* predicted movement time, it did not uniquely predict the dynamics and kinematics associated with the task performances.

Results

What participants do in a Fitts' task typically (slightly) deviates from the imposed task constraints. That is, the produced end-point variability and movement amplitude do not map one-to-one onto the task-defined target width *W* and distance *D*. As commonly done, we therefore computed the effective amplitude and the effective target width (see Methods) and calculated the effective *ID* as $ID_e = \log_2(2A_e/W_e)$. We report our results based on the ID_e.

As a first step in our analysis, we examined how *MT* changed under the different experimental factors. *MT* was lower in the discrete task (mean ± SD = 0.75 ± 0.04) than in the cyclic task (mean ± SD = 0.80 ± 0.04; $F(1,12) = 10.270$, $p < .01$, $\eta^2 = .461$) and higher in the distance manipulation (mean ± SD = 0.82 ± 0.05) than in width manipulation (mean ± SD = 0.73 ± 0.03; $F(1,12) = 23.975$, $p < .0001$, $\eta^2 = .666$). The Task × Manipulation interaction ($F(1,12) = 22.203$, $p < .005$, $\eta^2 = .649$) showed, however, that the effect of Task only held for the distance manipulation (Fig. 1a). As expected, *MT* increased with ID_e ($F(1.449,17.383) = 148.827$, $p < .0001$, $\eta^2 = .925$), but did so in a manner that interacted with Task ($F(2.903,34.842) = 18.228$, $p < .0001$, $\eta^2 = .603$; Fig. 1b), and Task and Manipulation

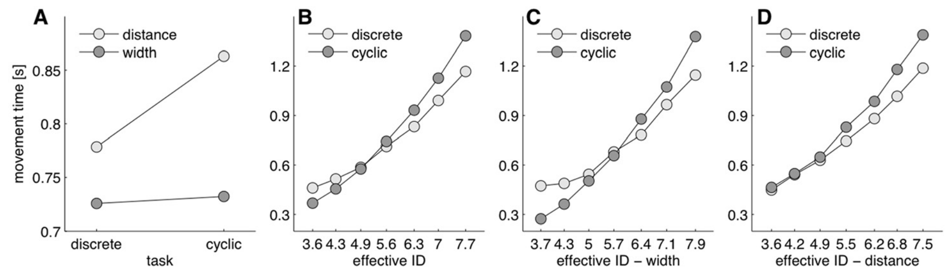

Fig. 1 Average movement time. **a** *MT* is lower in the discrete than in the cyclic task in the distance but not in the width conditions. **b** At low ID_e *MT* is higher in the discrete task than in the cyclic task, while at higher ID_e this is inversed. **c** This effect owes largely to the width conditions. **d** For distance, the cyclic *MT* equals the discrete *MT* at low ID_e but is (again) higher at high ID_e

($F(2.770,33.236) = 3.376$, $p < .05$, $\eta^2 = .220$; Fig. 1c, d). For each task and manipulation combination, we linearly regressed *MT* against effective *ID* (for each participant), and investigated the regressions' slopes with a 2 (Task) × 2 (Manipulation) ANOVA. The average R^2 equalled .91 (±0.08). The slopes in the discrete task (mean ± SD = 0.19 ± 0.01) were smaller than in the cyclic task (mean ± SD = 0.24 ± 0.02; $F(1,12) = 56.856$, $p < .0001$, $\eta^2 = .826$), and those in distance conditions (mean ± SD = 0.18 ± 0.01) were smaller than those in the width conditions (mean ± SD = 0.24 ± 0.02; $F(1,12) = 75.028$, $p < .0001$, $\eta^2 = .862$). The significant Task × Manipulation interaction ($F(1,12) = 6.929$, $p < .05$, $\eta^2 = .366$) indicated that the effect of Manipulation was stronger in the cyclic task (mean ± SD = 0.20 ± 0.02 versus 0.28 ± 0.02 for distance and width scaling, respectively) than in the discrete task (mean ± SD = 0.16 ± 0.01 versus 0.19 ± 0.01 for distance and width scaling, respectively). Thus, both the task version (discrete, cyclic) and how *ID* was varied (via *D* or *W*) altered the rate of *MT* increase with ID_e. At the same time, as a first approximation, the linear relation predicted by Fitts' law held in all Task × Manipulation conditions.

To investigate the dynamics associated with the movements in the various conditions, we computed the vector fields, and statistically analysed the maximal angle θ_{max} [17]. In that regard, each vector k in a vector field has (up to) eight neighbouring vectors whose direction relative to vector k can be represented by an angle. θ_{max} represents the maximum of the angles of vector k with its neighbouring vectors. For $\theta_{max} > 90°$, we consider that the movements in the corresponding trial pertained to a fixed-point dynamics. In almost all conditions, except for the cyclic-width condition at a low ID_e and for a few trials in the cyclic-distance condition, indications for the existence of fixed points in the target regions were found (see Fig. 2 and Table 1). This observation was statistically corroborated by the ANOVA on θ_{max} (Additional file 1), which indicated that θ_{max} was higher in the discrete task (mean ± SD = 171° ± 0.6) than in the cyclic one (mean ± SD = 130° ± 3.5; $F(1,12) = 123.893$, $p < .0001$, $\eta^2 = .912$), and higher in the distance conditions (mean ± SD = 160° ± 2.3) relative to those of width (mean ± SD = 142° ± 1.4; $F(1,12) = 99.556$, $p < .0001$, $\eta^2 = .892$). As expected, θ_{max} became larger as ID_e increased ($F(3.765,45.180) = 28.289$, $p < .0001$, $\eta^2 = .702$). The distance versus width effect, however, was only observed for the cyclic task (Task × Manipulation, $F(1,12) = 54.782$, $p < .0001$, $\eta^2 = .820$). In addition, the increase of θ_{max} with ID_e occurred primarily in the width (Manipulation × ID_e, $F(3.010,36.126) = 18.737$, $p < .0001$, $\eta^2 = .610$) and in the cyclic conditions (Task × ID_e, $F(3.552,42.267) = 43.048$, $p < .0001$, $\eta^2 = .782$). Finally, the Task × Manipulation × ID_e interaction ($F(3.022,36.261) = 9.456$, $p < .0001$, $\eta^2 = .441$) showed that θ_{max}

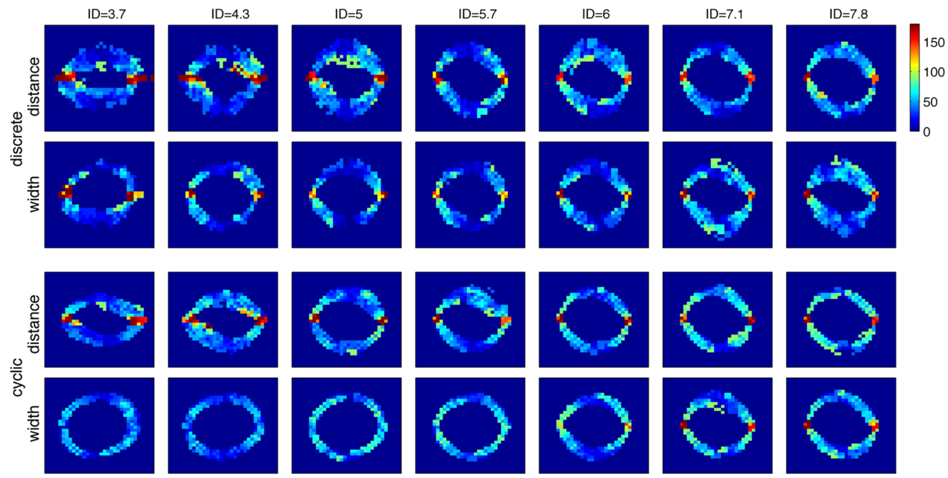

Fig. 2 Angle diagrams. The upper versus lower two rows represent angle diagrams from a single participant of the discrete and cyclic mode, respectively. For both row pairs, the upper panels show the distance conditions while the lower ones display the width conditions. ID_e increases form left to right. The colour coding (at the right) represents the maximal angle between neighbouring vectors. Red areas indicate locally opposing angles, implying the existence of a fixed point. Their absence suggests the existence of a limit cycle

was high (>130°) and varied little only with ID_e in all task–manipulation combinations except for that of cyclic–width. As can be seen in Table 1 (see also Additional file 2), the number of participants in which fixed points were identified (in correspondence with the criterion outlined above) always equalled the total number of participant (i.e., $n = 13$) in all discrete task conditions. In the cyclic-discrete task conditions, fixed points were always found for the higher ID_e. However, all but one (2 ID_e) or 3 participants (1 ID_e) did not show a fixed-point dynamics at low ID_e. Two of the participants that did not adhere to a fixed-point dynamics at $ID_e = 4.9$ were 'stand-alone' incidences. In one participant no fixed points were found for the first three ID_e's, that is, this participant's behaviour in all likelihood showed a true transition. In the cyclic-width task conditions, all participants showed a transition from a limit cycle dynamics to a fixed points dynamics with increasing ID_e, albeit at different ID_e. Thus, across the board (with a single exception), a limit cycle dynamics was operative in the cyclic–width condition at ID_e up to about 5.6, whereas a fixed-point dynamics governed all other conditions.

Topologically, the vector fields of all conditions in which a fixed-point dynamics was identified were indistinguishable. For cyclic Fitts' task performance the gradual up-scaling of task difficulty, in particular through manipulation of target width, gradually increases the degree

Table 1 Number of participants for whom fixed points were identified per condition

		IDe						
		3.6	*4.3*	*4.9*	*5.6*	*6.3*	*7.0*	*7.7*
Task	*Manipulation*							
Discrete	Distance	13	13	13	13	13	13	13
	Width	13	13	13	13	13	13	13
Cyclic	Distance	12	12	10	13	13	13	13
	Width	0	0	2	7	12	13	13

of the system's nonlinearity [11]. Fig. 2 suggests that this was also the case for the discrete task performances (see also [12]). The degree of nonlinearity does not uniquely map onto a system's topological organization. Its evolution as a function of ID_e, however, informs about the quantitative changes in the movement dynamics. We summarize these changes via $R_{AT/MT}$, which quantifies the degree of symmetry of the movement velocity profile. $R_{AT/MT}$ was lower in the discrete task (mean ± SE = 0.35 ± 0.02) than in the cyclic task (mean ± SD = 0.39 ± 0.04; $F(1,12) = 28.982$, $p < .0001$, $\eta^2 = .707$), but primarily so in the width conditions (Task × Manipulation ($F(1,12) = 53.321$, $p < .0001$, $\eta^2 = .816$; Fig. 3a). In line therewith, $R_{AT/MT}$ was lower in the distance manipulation (mean ± SD = 0.34 ± 0.02) than in that of the width manipulation (mean ± SD = 0.39 ± 0.01; $F(1,12) = 36.564$, $p < .0001$, $\eta^2 = .753$). At first glance, this latter finding appears to contradict established knowledge [7, 11, 12, 27]; it is important to recall therefore, that in the present distance manipulation, the fixed target width was always very small (0.31 cm). As expected, $R_{AT/MT}$ decreased as ID_e increased ($F(2.205,26.458) = 136.922$, $p < .0001$, $\eta^2 = .919$). This decrease was stronger for discrete than for the cyclic conditions, and at high ID_e the task mode differences vanished (Task × ID_e; $F(2.908,34.899) = 14.305$, $p < .0001$, $\eta^2 = .544$; Fig. 3b). Similarly, the interaction between Manipulation and ID_e ($F(2.068,24.822) = 42.956$, $p < .0001$, $\eta^2 = .782$) indicated that the manipulation differences vanished with increasing ID_e. Finally, the Task × Manipulation × ID_e interaction ($F(3.625,43.504) = 7.302$, $p < .0001$, $\eta^2 = .378$) indicated that $R_{AT/MT}$ decreased faster in the cyclic than in the discrete task mode with increasing ID_e for the width conditions but not so for the distance conditions (Fig. 3c, d). Thus, the velocity profiles became more skewed with increasing ID_e (i.e., the nonlinearity increased). Whereas this effect was similar for both tasks in the distance manipulation, for the width manipulation, the profiles were more symmetric at low ID_e in the cyclic task than in the discrete task. This latter difference vanished as in both task modes the profiles became more asymmetric (i.e., the movements became more nonlinear).

As indicated in the *Background* section, we expected that under the distance manipulation at low *ID* a driven fixed point would govern the movements. In such a dynamic system, the phase space trajectories can be expected to be wiggly (and show little local convergence), and thus to be variable from one trial to the next. We therefore examined the trajectory variability using PCA (see also Additional file 3), and subjected the first eigenvalue to an ANOVA. Please note that the more variable the trajectories are, the smaller the first eigenvalue is. In fact, the variance that is not accounted for by the

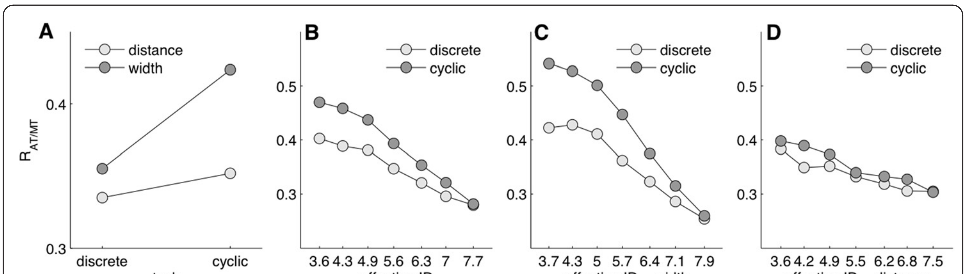

Fig. 3 Ratio AT/MT. **a** The larger $R_{AT/MT}$ in the width condition relative to the distance conditions is most pronounced in the cyclic task mode. **b** At low ID_e $R_{AT/MT}$ is lower in the discrete task than in the cyclic task, while at higher ID_e $R_{AT/MT}$ is similar. **c** This interaction is due to the width conditions. **d** In the distance conditions $R_{AT/MT}$ is similar and decreasing with ID_e for both task modes

first principal component is orthogonal to it so that the first eigenvalue can be interpreted as reflecting the degree of convergence towards the trajectory associated with the first principal component. Neither the effect of Task nor that of ID_e was significant ($p > .1$ and $p > .05$, respectively). In contrast, the trajectories were more variable (i.e., the 1st eigenvalue smaller) in the distance conditions (mean ± SE = .76 ± 0.01) than in those of width (mean ± SE = .84 ± 0.01; $F(1,12) = 140.683$, $p < .0001$, $\eta^2 = .921$). The Task × Manipulation interaction ($F(1,12) = 17.132$, $p < .0005$, $\eta^2 = .588$) indicated that the difference between task manipulations was larger in the cyclic task mode than in the discrete one. The significant interaction between Task and ID_e ($F(3.374,40.486) = 26.453$, $p < .0001$, $\eta^2 = .688$), Manipulation and ID_e ($F(2.713,32.559) = 43.106$, $p < .0001$, $\eta^2 = .782$), and Task, Manipulation and ID_e ($F(3.061,36.734) = 7.385$, $p < .005$, $\eta^2 = .381$) are displayed in Fig. 4. In combination, these interactions showed that at low ID_e, the trajectory variability in the discrete task was larger than that of the cyclic task, which inversed at high ID_e (Fig. 4a). Further, the trajectories were most variable at low ID_e in the distance manipulation, and the variability decreased as ID_e increased (Fig. 4b), The inverse was observed for the width conditions. The effect of increasing ID via target distance was comparable for both tasks (Fig. 4c, d). Decreasing target width, however, hardly affected the trajectory variability in the discrete task, but it led to an increased variability in the cyclic task. For the latter, at low ID_e, that is, when a limit cycle dynamics was invariantly present, the trajectories were the least variable in the entire dataset.

As for the movement organization under the different conditions, our results revealed identical topological organizations (fixed-point dynamics) under all but the cyclic-width task version at low ID_e (and for one participant in the cyclic-distance task at low ID_e). At the same time, however, the discrete and cyclic task modes are set apart in terms of the degree of symmetry of movement velocities, and particularly, trajectory variability. By hypothesis, this distinction may imply that in the cyclic task mode, the dynamical organization (i.e., the phase flow) remains invariant throughout the entire trial, independent of whether a fixed-point or limit cycle dynamics is adhered to. For the discrete task mode, this will actually be the same. In this case, however, prior to and following each single aiming the movement-task organization will be (has to be) 'dismantled' (to return to the home position) and assembled for the execution of the next trial. Consequently, additional performance variability can be expected for the discrete task mode relative to the cyclic one as the trial-to-trial re-establishment of the movement organization adds a source of variability for the former

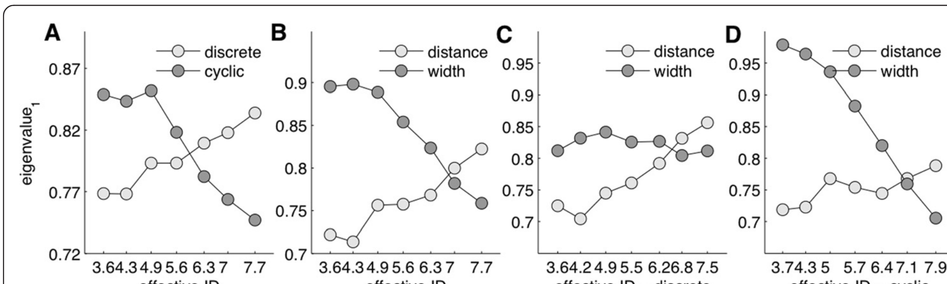

Fig. 4 PCA: 1st eigenvalue. **a** Trajectory variability decreased with increasing ID_e for the discrete task mode whereas it increased in the cyclic mode (from the 3rd ID_e onwards). **b** Similarly, trajectory variability in the distance conditions decreased with increasing ID_e whereas that in the width conditions increased. **c**, **d** This effect, however, was most pronounced for the cyclic task. In the discrete task trajectory variability in the width condition stayed about the same for all ID_e

task mode relative to the latter. In terms of Saltzman and Munhall's [32] wording, additional variability in repeated discrete aiming relative to continuous cyclic aiming is introduced in terms of parameter dynamics. We tested this hypothesis by focussing on the variability (through the coefficient of variation) of the variable central to Fitts' law, that is movement time. Consistent with the hypothesis, the movement time's coefficient of variation (CV_{MT}) was larger in the discrete task (mean ± SD = 1.18 ± 0.01) than in the cyclic one (mean ± SD = 1.12 ± 0.01; $F(1,12) = 63.735$, $p < .0001$, $\eta^2 = .842$), and also larger in the distance conditions (mean ± SD = 1.16 ± 0.01) than in the width conditions (mean ± SD = 1.13 ± 0.01; $F(1,12) = 43.829$, $p < .0001$, $\eta^2 = .785$). This latter effect was stronger in the cyclic than in the discrete task (Task × Manipulation; $F(1,12) = 5.271$, $p < .05$, $\eta^2 = .305$; Fig. 5a). Further, CV_{MT} decreased with increasing ID_e ($F(4.306,51.667) = 6.812$, $p < .0001$, $\eta^2 = .362$); this effect, however, was confined to the discrete task (Task × ID_e; $F(3.201,38.417) = 7.810$, $p < .0001$, $\eta^2 = .394$; Fig. 5b). Finally, the interaction between Manipulation and ID_e ($F(3.526,42.317) = 55.529$, $p < .0001$, $\eta^2 = .822$) indicated that at low ID_e, the CV_{MT} under the distance manipulation, which decreased strongly as ID_e increased, was almost twice as high as that under the width manipulation, which increased moderately as ID_e increased (Fig. 5c).

The pattern of intra-participant $R_{AT/MT}$ variability (coefficient of variation) strongly resembled that of CV_{MT}, and is reported in Additional file 4.

Discussion

In the present study, we investigated both the dynamics and kinematics underlying Fitts' task performance during discrete and cyclic task modes when *ID* was varied through distance and width independently. Most importantly regarding the dynamics, consistent with previous observations [17], in the cyclic task setting a transition from a limit cycle to a fixed-point dynamics occurred when scaling the *ID* via target width. In contrast to the expectation voiced in that study, a similar transition was not observed here when varying *ID* via the distance separating the targets. Indeed, varying target distance did not affect the observed movement's topology, at least not in the presently studied range. In this case, fixed points were found throughout the entire *ID* range (except for a few cases, mainly one participant). This result suggests that, in general, the index of difficulty per se does not uniquely dictate the dynamical organization of rapid aiming movements, thereby disqualifying as a bifurcation parameter. That function,

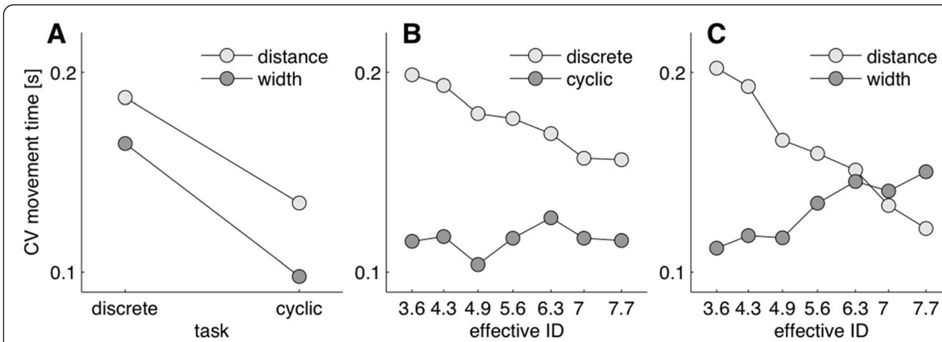

Fig. 5 CV movement time. **a** The distance-width CV_{MT} difference is moderately stronger in the cyclic than in the discrete task mode. **b** In the discrete task CV_{MT} increases with ID_e whereas in the cyclic task it decreases. **c** In the distance conditions CV_{MT} decreases with increasing ID_e whereas in the width conditions it increases

however, appeared to be fulfilled by target width, even though only so for the cyclic task mode. Indeed, varying target distance did not affect the movement's topology observed, at least not in the presently studied range. It cannot be ruled out, however, that the smallness of the target (0.31 cm) under the present distance manipulations hindered the occurrence of a limit cycle dynamics (or any other; see below) at specific target distances.

Furthermore, trajectory variability changed in opposing direction with decreasing target width for the discrete and cyclic task. This observation seems hard to reconcile with the idea that the kinematic re-organization as a function of (varying) target width for both task modes is the same. That is, even if varying target width drives the sensorimotor system through a bifurcation when operating in the discrete task mode, it is unlikely that the bifurcation type matches the one observed in the cyclic task. Confirmation (or not) of this hypothesis, however, will require further investigation.

Concerning the effects on the movement kinematics, we found that how *ID* was varied (i.e., via *D* or *W*) as well as the nature of the task (i.e., discrete or cyclic) had pronounced effects on the movement kinematics investigated. In that regard, it is often stated that scaling target distance versus its width 'simply' stretches the velocity profile or skews it, respectively [7, 11, 12]. Here, we found that although increasing the *ID* by scaling target width reduced the degree asymmetry of the movement's velocity profile more than under the distance scaling, the latter also reduced it (Fig. 3b). Again, this may to some extent be due to the smallness of the target under the present distance scaling. By comparison, we here used a target width smaller than the one used in [12] and [11] under a (modestly; relative to [10]) larger distance scaling. A closer look at these studies, however, shows that while, indeed, the degree of asymmetry increases markedly more under the width than distance scaling, categorically setting apart the effects of these variations in terms of skewing versus stretching the velocity profiles appears a simplification that does not do justice to the observations.

Further, the degree of asymmetry increased with decreasing target width. In that case, at low *ID*, the discrete movements were more asymmetric than the cyclic ones, while at high *ID*, this difference vanished as for both task modes the asymmetry increased. The initial difference, as well as the evolution, can be understood when considering that discrete movements always contain a zero velocity and acceleration start and end points, which emerge at higher *ID* only for cyclic movements. Indeed, under the distance scaling, the symmetry reduction was similar for the discrete and cyclic task mode (Fig. 3d), which was always governed by a fixed-point dynamics.

The effects of varying target distance versus width were not limited to the movement's velocity symmetry. Specifically, increasing target distance (under constant target width) reduced the movement's trajectory variability irrespective of task mode. As peak velocity also increases with increasing distance (Additional file 5), this effect contrasts the signal-dependent noise perspective [33]. Reasoning from a dynamical perspective, and assuming noise to be approximately constant, a reduction in trajectory variability may come about by an increased (more or less local) convergence of the phase flows underlying the movements (i.e., an increased tendency of the vectors pointing towards a manifold in the state space) and/or by an increased contribution of the deterministic dynamics relative to the stochastic dynamics (i.e., an increased length of the vectors). Under this perspective, increasing the *ID* via target distance is likely to result in an increased flow convergence for both task modes, which indeed occurs (reduced trajectory variability; see Fig. 2 and Additional file 3). The marked reduction in inter-aiming movement time variability (CV_{MT}; Fig. 5c) is consistent therewith. In contrast, varying *ID* via target width did not (globally) affect the trajectory variability in the discrete task mode, but resulted in a marked variability increase in the cyclic task mode: In these conditions, at low *ID* and governed by a limit cycle dynamics, trajectory variability was the lowest observed but it noticeably (but rather gradually) increased as the non-linearity increased ($R_{AT/MT}$; Fig. 3d) and a fixed point dynamics was created (Fig. 2).

We found support for the hypothesis that the variability across aiming movements is bigger in the discrete task mode than in the cyclic one. This might result from the dynamical organization (i.e., the phase flow) being more or less invariant throughout the entire trial, depending on the type of task: in the discrete task mode, the perceptual-motor system prepares the movement for each upcoming action (leading to more variability) while across repeated aiming movements (in the cyclic task mode), the dynamical organization is more invariant (less variable). To further investigate this interpretation, we calculated the Pearson correlation for the movement time variability (CV_{MT}) between all Task, Manipulation, and low and high *ID* condition pairs (NB: in order to obtain more data points, the lowest two *ID* conditions and the highest two *ID* conditions were taken together to form a 'low *ID*' and 'high *ID*' category). Our reasoning was that, if tasks share specific processes relevant for their (timed) behaviour, their variability ought to be correlated and, conversely, if not, no correlation is to be expected [34]. Accordingly, we expected that all correlations between pairs involving a discrete and cyclic condition would be non-significant, and that for the cyclic task the low *ID* – width condition would show no significant correlation with any of the others as the dynamics in the former condition (limit cycle) differed from the latter (fixed points).

As it can be appreciated in Fig. 6, these expectations turned out to be correct. Further, for the rhythmic task, all pairs except for those involving the low *ID* – width condition turned out significant, which fits the observation of similar dynamics (fixed points) and the proposition of being governed by an invariant dynamics across repetitive aiming movements. For the discrete task, however, the correlations were less straightforward: the CV_{MT} of multiple pairs correlated, but not all did, and the 2×2 matrix was not symmetric. We therefore abstain from any further interpretations.

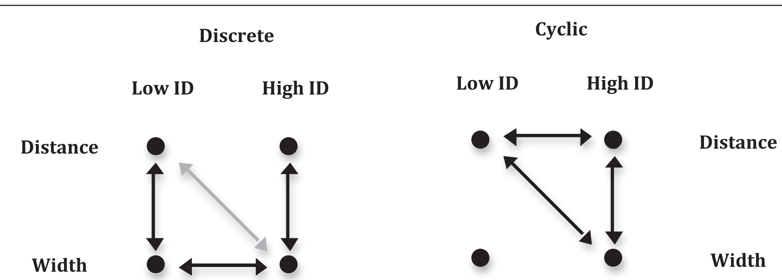

Fig. 6 Pearson's correlation *r* for CV_{MT} between conditions. Black arrows indicate significant correlations ($p < .05$; across correlations $.41 < r < .70$), the grey arrow indicates a marginal significant correlation ($.1 < p < .05$; $r = .36$). The absence of arrows indicates that the correlation was not significant. No correlations between any of the discrete and cyclic conditions were found; within the cyclic task mode, no correlation was found between the low *ID* – width condition and the others. For the discrete task mode, several significant correlations were identified

As discussed above, we found evidence that in a subset of these combinations limit cycle dynamics were observed, while in another subset, fixed points regimes were found. Some indications (not conclusive) were found that the nature of the fixed points might have been dissimilar in the later subset dependent on the experimental factors. Regardless, in all task and manipulation combinations, movement time increased as the *ID* increased. That is, this trade-off appeared independent of the dynamical organization underlying Fitts' task performance. The question then arises of what could be the origin of the increase of *MT* with *ID*? The different models available in the literature do not provide satisfying answers in this respect. For instance, the dynamical model proposed by Mottet and Bootsma [11] fails for discrete movements—for these an *N*-shape in the Hooke plane appears independent of *ID*. Similarly, models from the 'corrective (sub) movements class' ([5, 14]; see *Background*) fail to deal with performances in (at least a large part of) the limit cycle regime since no corrective sub-movements are made (acceleration is about highest around the targets, [11]) but *MT* still gets larger with increasing *ID*. That is, while both models have their merits in their respective domains, neither of them is able to explain the *MT* increase with increasing *ID* across the range of task conditions that is reported here, and in the literature more at large.

Conclusions

Consistent with the Fitts' law, movement time scaled (approximately) linearly with the index of difficulty *ID* under all task and manipulation conditions. However, the system's functional organization underlying task performance differed both qualitatively and quantitatively as a function of task mode (cyclic vs. discrete) and manipulation (*D* vs. *W*). Within the cyclic task mode, low *ID*s were associated with limit cycles or fixed points dependent on whether target width or distance was manipulated, respectively. In this respect, target width was the parameter causing a bifurcation at a critical value. Conversely, for the discrete task mode, we did not observe such a bifurcation. Both behavioural modes adhere to distinct functional organizations; for instance velocity and acceleration always have to vanish at the target in discrete task mode. Consistent herewith, analysis of movement time variability (CV_{MT}) set apart the discrete and cyclic task mode, even for IDs in which both task modes appeared governed by a fixed-point dynamics. We argue that their difference is due to the inherent need for the perceptual-motor system to instantiate every single aiming in the discrete but not cyclic task mode, thereby introducing variability at another level of the perceptual-motor organization (i.e., that of the parameter dynamics; [32]). In addition, it cannot be ruled out that the nature of the fixed-points, or the space within which they exist, is dissimilar across both task modes and *ID*-manipulations. While our present data do not allow us to either conclusively refute or confirm this hypothesis, the differential trajectory variability evolution as a function of the task modes and distance versus width manipulation provides a hint thereto.

Regardless, the functional organization underlying task performance at various *ID*s varied markedly as a function of task mode and manipulation. In fact, our results counter the idea that change in a single parameter (as a function of *ID*) of the dynamics and/or bifurcation structure can account for Fitts' law. Explanations in terms of correction strategies, however, as discussed above, also have their limitations. That is, explaining Fitts' law in terms of a single dynamical organization or movement strategy remains problematic. In fact, this may indicate that a full description of Fitts' law may require more than one control (or bifurcation) parameter. The remaining question, then, is which one? We found evidence that target width, rather than task difficulty, acts as a control parameter. No clear indication was found that target distance did so too (except for a single participant) even though changing target distance had the opposite effect (of width) on trajectory variability. This may be due to a differential effect of the degree of convergence of the phase flow for both parameters. This, however, is of yet an open question. Regardless, this discussion resonates with previously expressed doubts as to whether the notion of task difficulty as quantified through target distance divided by width is appropriate. For instance, Welford and colleagues proposed a definition incorporating two additive logarithmic D and W terms [8]. Further, task difficulty is insensitive to energetic cost [35], which is higher at the easy task difficulty spectrum. Also, anecdotal reports from our participants suggest that subjective difficulty does not map uniquely onto the index of difficulty (the low *ID* small width-small distance conditions were experienced as particularly difficult). That is, the explicit identification of the nature of the fixed points in the various task conditions as well as the control parameter(s) implicated seems of a particular interest for the Fitts' paradigm. If a second control parameter indeed exists, its identification may well alter the notion of task difficulty as currently understood.

Methods

Thirteen (self-declared) right-handed participants (7 females; age: 29.3 ± 3.8 years) performed aiming movements from a starting point to a target (discrete mode) or between two targets (cyclic mode) with a hand-held stylus (18 g, 156.5×14.9 mm, ~1 mm tip) across a digitizer tablet (Wacom Intuos XL, 1024×768 pixel resolution) under instructions stressing both speed and accuracy. Position time series were acquired from the tablet via custom-made software (sampled at 250 Hz). The targets were printed in red on white A3 paper that was positioned under the transparent sheet of the tablet. In the cyclic mode, for each condition two trial repetitions consisting of 50 horizontal reciprocal aiming movements each (i.e., 25 cycles) were performed in the transversal plane, once starting from the left target and once from the right target. In the discrete mode, four blocks consisting of 25 single aiming movements were performed twice; in two blocks movements were made toward a target positioned on the right side; in the two other blocks the direction was inversed. Cyclic trials with more than 6 errors and discrete blocks with more than 3 errors were redone (i.e., a 12% error rate was tolerated). In both task modes target distance and target width were manipulated independently, and chosen so as to allow for a large sampling of distance and width, respectively. In the width manipulation, target distance was set at 20 cm, and target width varied as follows: 4.20, 2.50, 1.49, 0.88, 0.53, 0.31, and 0.19 cm. In the distance manipulation, target width was set at 0.31 cm, and target distance was varied from 1.47, 2.48, 4.17, 7.01, 11.80, 19.84, and 33.37 cm. In both cases, this resulted in seven *ID*s (from 3.25 to 7.75, step size 0.75), which were administered randomly. Participants were familiarized with all task mode (discrete, cyclic) by manipulation (distance, width) conditions by performing 5 to 10 movements (until fast and successful performance) with $ID = 3.25$ and $ID = 7.00$. The familiarization ended when the participant reached a stable behaviour (i.e., moving fast and not missing the target). The width and distance manipulations were assessed in two experimental sessions lasting about 1½ hour each. Both the width and distance manipulations, as well as the cyclic and discrete tasks were counterbalanced across participants.

For the rhythmic movements, the peaks in the (horizontal) position time series were taken as movement initiations and terminations. The discrete movements' initiation and termination were defined as the moment its (absolute) velocity exceeded versus fell below 0.1 cm/s, respectively. For the termination, the additional criterion was used that the movement velocity had to remain below this velocity criterion for minimally 60 ms [5]. A secondary movement was deemed present if it lasted for minimally 100 ms, the velocity criterion was exceeded for at least half of the burst's time, and if the covered distance was minimally either 2 mm or ¼ of the target width. If present, the secondary movement's endpoint was taken as the movement's termination. (For movement time, we verified whether the inclusion of the secondary movement changed the patterns of results, which was not the case.) Movement time (*MT*) was defined as the average of the temporal differences between movement termination and onset. For each movement, the acceleration duration (*AT*) was defined as the moment of peak velocity minus movement initiation. The ratio *AT/MT* ($R_{AT/MT}$) measures of the degree of symmetry of the movement velocity's profile. Effective amplitude (A_e) was computed as the average distance traversed across repetitions, and effective target width (W_e) as 2×1.96 times the mean standard deviation at the movement terminations [36]. Next, effective *ID* was calculated as $ID_e = \log_2(2A_e/W_e)$.

In order to reconstruct the vector field underlying the movements [37, 38], we computed the conditional probability distributions $P(x,y,t|x_0,y_0,t_0)$ that indicated the probability to find the system at a state (x,y) at a time t given its state (x_0, y_0) at an earlier time t_0. These distributions were computed using all aiming movements in each condition using a grid size of 28 bins. Drift coefficients (i.e., the deterministic dynamics) were computed according to:

$$D_x(x,y) = \lim_{\tau \to 0} \frac{1}{\tau} \iint (x' - x) P(x', y', t + \tau | x, y, t) dx' dy$$

$$D_y(x,y) = \lim_{\tau \to 0} \frac{1}{\tau} \iint (y' - y) P(x', y' t + \tau | x, y, t) dx' dy$$

These coefficients are the numerical representations of the *x*-, and *y*-component of the vector at each phase space position. From these coefficients, we computed the angle θ_{max} for each bin between its corresponding vector and that of each of its neighbours (if existent), and extracted the corresponding maximal value in order to visualize the phase flows in terms of so-called angle diagrams [17, 39].

We performed a principal component analysis (PCA) to investigate trajectory variability (x,y). For each participant and condition all trajectories were resampled to 100 samples, and subjected to principal component analysis [17]. A PCA was done separately for the 50 left-to-right and 50 right-to-left aiming movements. The 1st eigenvalue λ_1 was next averaged.

The ANOVA on ID_e showed multiple effects, we therefore created ID_e block averages of *MT*, $R_{AT/MT}$, θ_{max}, and λ_1 that were subjected to a repeated measures ANOVA with *Task* (2), *Manipulation* (2), and ID_e (7) (i.e., a total of 28 conditions) as within participant factors. The Greenhouse-Geisser correction was applied whenever necessary. Significant main effects (α = .05) were followed up by Bonferroni-corrected post hoc tests. (For completeness, the same analyses were performed for peak velocity, acceleration, and deceleration time; they are reported in Additional file 5, 6, 7, respectively).

The protocol was in agreement with the Declaration of Helsinki. Informed consent was obtained from all participants prior to the experiment.

Additional files

Additional file 1: Maximal vector field angles θmax.

Additional file 2: Classification of dynamics for the cyclic task.

Additional file 3: Phase plane trajectories and their variability.

Additional file 4: Intra-participant RAT/MT variability CV RAT/MT.

Additional file 5: Peak velocity (PV).

Additional file 6: Acceleration time (AT).

Additional file 7: Deceleration time (DT).

Competing interests
The author(s) declare that they have no competing interests.

Authors' contributions
All authors designed the study. HK and RSM conducted the experiment. RH, HK, and RSM analyzed the data. RH wrote the manuscript. All authors wrote, improved and approved the final manuscript.

Acknowledgement
The research here reported was support by the French Centre National de la Recherche Scientifique.

Author details
[1]Institut de Neurosciences des Systèmes, INSERM UMR1106, Aix-Marseille Université, Faculté de Médicine, la Timone, 27 Bd Jean Moulin, 13005 Marseille, France. [2]Aix-Marseille Université, CNRS, Institut des Sciences du Mouvement UMR 7287, 13288, 13009 Marseille, France.

Received: 4 May 2015 Accepted: 2 July 2015
Published online: 12 August 2015

References
1. Fitts PM. The information capacity of the human motor system in controlling the amplitude of movement. J Exp Psychol. 1954;47(6):381–91.
2. Fitts PM, Peterson JR. Information capacity of discrete motor responses. J Exp Psychol. 1964;67(2):103–12.
3. Shannon C, Weaver W. The mathematical theory of communication. Urbaba, IL: University of Illinois Press; 1949.
4. MacKenzie IS. Fitts' law as a research and design tool in human-computer interaction. Human-Computer Interaction. 1992;7:91–139.
5. Meyer DE, Kornblum S, Abrams RA, Wright CE, Smith JEK. Optimality in human motor-performance - ideal control of rapid aimed movements. Psychol Rev. 1988;95(3):340–70. doi:10.1037/0033-295x.95.3.340.
6. Schmidt RA, Zelaznik H, Hawkins B, Frank JS, Quinn JT. Motor-output variability - theory for the accuracy of rapid motor acts. Psychol Rev. 1979;86(5):415–51. doi:10.1037//0033-295x.86.5.415.
7. Guiard Y. The problem of consistency in the design of Fitts' law experiments: consider either target distance and width or movement form and scale. ACM Conference on Human Factors in Computing Systems. New York: Sheridan Press; 2009. p. 1908–18.
8. Welford AT, Norris AH, Shock NW. Speed and accuracy of movement and their changes with age. Acta Psychol. 1969;30:3–15.
9. Buchanan JJ, Park JH, Shea CH. Target width scaling in a repetitive aiming task: switching between cyclical and discrete units of action. Exp Brain Res. 2006;175(4):710–25. doi:10.1007/S00221-006-0589-1.
10. Guiard Y. Fitts' law in the discrete vs cyclical paradigm. Hum Movement Sci. 1997;16(1):97–131. doi:10.1016/S0167-9457(96)00045-0.
11. Mottet D, Bootsma RJ. The dynamics of goal-directed rhythmical aiming. Biol Cybern. 1999;80(4):235–45. doi:10.1007/S004220050521.
12. Sleimen-Malkoun R, Temprado JJ, Huys R, Jirsa V, Berton E. Is Fitts' Law continuous in discrete aiming? Plos One. 2012;7(7):e41190. doi:10.1371/journal.pone.0041190.
13. Smits-Engelsman BC, Swinnen SP, Duysens J. The advantage of cyclic over discrete movements remains evident following changes in load and amplitude. Neurosci Lett. 2006;396(1):28–32. doi:10.1016/j.neulet.2005.11.001.
14. Crossman ERFW, Goodeve PJ. Feedback control of hand-movement and Fitts' law. Q J Exp Psychol. 1963;35A:407–25.

15. Bongers RM, Fernandez L, Bootsma RJ. Linear and logarithmic speed-accuracy trade-offs in reciprocal aiming result from task-specific parameterization of an invariant underlying dynamics. J Exp Psychol Human. 2009;35(5):1443–57. doi:10.1037/A0015783.
16. Guiard Y. On Fitts and Hooke laws - simple harmonic movement in upper-limb cyclical aiming. Acta Psychol. 1993;82(1–3):139–59. doi:10.1016/0001-6918(93)90009-G.
17. Huys R, Fernandez L, Bootsma RJ, Jirsa VK. Fitts' law is not continuous in reciprocal aiming. P Roy Soc B-Biol Sci. 2010;277(1685):1179–84. doi:10.1098/Rspb.2009.1954.
18. van Mourik AM, Daffertshofer A, Beek PJ. Extracting global and local dynamics from the stochastics of rhythmic forearm movements. J Mot Behav. 2008;40(3):214–31. doi:10.3200/JMBR.40.3.214-231.
19. Strogatz SH. Nonlinear dynamics and chaos: with applications to physics, biology, chemistry, engineering. Cambridge Massachusetts: Perseus Books Publishing, LLC; 1994.
20. Haken H, Kelso JAS, Bunz H. A theoretical-model of phase-transitions in human hand movements. Biol Cybern. 1985;51(5):347–56. doi:10.1007/Bf00336922.
21. Kay BA, Saltzman EL, Kelso JAS, Schöner G. Space-time behavior of single and bimanual rhythmical movements - data and limit-cycle model. J Exp Psychol Human. 1987;13(2):178–92. doi:10.1037//0096-1523.13.2.178.
22. Daffertshofer A, van Veen B, Ton R, Huys R. Discrete and rhythmic movements - just a bifurcation apart? IEEE International Conference on Systems, Man and Cybernetics; San Diego. CA: IEEE; 2014. p. 778–83.
23. Kay BA. The dimensionality of movement trajectories and the degrees of freedom problem - a tutorial. Hum Movement Sci. 1988;7(2–4):343–64. doi:10.1016/0167-9457(88)90016-4.
24. Jirsa VK, Kelso JAS. The excitator as a minimal model for the coordination dynamics of discrete and rhythmic movement generation. J Mot Behav. 2005;37(1):35–51. doi:10.3200/Jmbr.37.1.35-51.
25. Schöner G. A dynamic theory of coordination of discrete movement. Biol Cybern. 1990;63(4):257–70. doi:10.1007/Bf00203449.
26. Buchanan JJ, Park JH, Shea CH. Systematic scaling of target width: dynamics, planning, and feedback. Neurosci Lett. 2004;367(3):317–22. doi:10.1016/J.Neulet.2004.06.028.
27. Thompson SG, McConnell DS, Slocum JS, Bohan M. Kinematic analysis of multiple constraints on a pointing task. Hum Movement Sci. 2007;26(1):11–26. doi:10.1016/J.Humov.2006.09.001.
28. Sleimen-Malkoun R, Temprado JJ, Berton E. Age-related changes of movement patterns in discrete Fitts' task. BMC Neurosci. 2013;14:145. doi:10.1186/1471-2202-14-145.
29. Perdikis D, Huys R, Jirsa VK. Complex processes from dynamical architectures with time-scale hierarchy. PLoS One. 2011;6(2):e16589. doi:10.1371/journal.pone.0016589.
30. Feldman AG. Once more on the equilibrium-point hypothesis (lambda-model) for motor control. J Mot Behav. 1986;18(1):17–54.
31. Kugler PN, Kelso JAS, Turvey MT. On the concept of coordinative structures as dissipative structures: I. Theoretical lines of convergence. Advances in psychology: Vol.1. Tutorials in motor behavior. Amsterdam, the Netherlands: Elsevier B.V; 1980. p. 3–47.
32. Saltzman EL, Munhall KG. Skill acquisition and development: the roles of state-, parameter, and graph dynamics. J Mot Behav. 1992;24(1):49–57. doi:10.1080/00222895.1992.9941600.
33. Harris CM, Wolpert DM. Signal-dependent noise determines motor planning. Nature. 1998;394(6695):780–4. doi:10.1038/29528.
34. Robertson SD, Zelaznik HN, Lantero DA, Bojczyk KG, Spencer RM, Doffin JG, et al. Correlations for timing consistency among tapping and drawing tasks: evidence against a single timing process for motor control. J Exp Psychol Human. 1999;25(5):1316–30. doi:10.1037/0096-1523.25.5.1316.
35. Guiard Y, Olafsdottir H, Perrault S, editors. Fitts' law as an explicit time/error trade-off. ACM Conference on Human Factors in Computing Systems, 2011.
36. Kostrubiec V, Zanone PG, Fuchs A, Kelso JAS. Beyond the blank slate: routes to learning new coordination patterns depend on the intrinsic dynamics of the learner-experimental evidence and theoretical model. Front Hum Neurosci. 2012;6:Artn 222. doi:10.3389/Fnhum.2012.00222.
37. Plamondon R, Alimi AM. Speed/accuracy trade-offs in target-directed movements. Behav Brain Sci. 1997;20(2):279–303.
38. Welford AT. Fundamentals of skill. London, UK: Methuen; 1968.
39. Peinke J, Friedrich R, Chilla F, Chabaud B, Naert A. Statistical dependency of eddies of different sizes in turbulence. Z Phys B Con Mat. 1996;101(2):157–9. doi:10.1007/S002570050194.
40. van Mourik AM, Daffertshofer A, Beek PJ. Estimating Kramers-Moyal coefficients in short and non-stationary data sets. Phys Lett A. 2006;351(1–2):13–7. doi:10.1016/J.Physleta.2005.10.066.
41. Huys R, Studenka BE, Rheaume NL, Zelaznik HN, Jirsa VK. Distinct timing mechanisms produce discrete and continuous movements. PLoS Comput Biol. 2008;4(4):Artn E1000061. doi:10.1371/Journal.Pcbi.1000061.